A New Approach to Model Frequency Dependent Network Equivalents in Transient Simulation Tools

Meysam Ahmadi, Aniruddha M. Gole

Abstract— **In this paper, utilizing *Brune's* realization method, a new approach introduced to fit the Frequency Dependent Electric Networks (FDNEs) responses by means of passive circuits containing RLC elements. In this approach, by taking simple steps the frequency response can be directly transferred to the time domain simulation without need of mathematical curve-fitting. The fitting process is a numerical implementation of the *Brune's* realization method and similar algorithm is used for the tabular functions of FDNEs. Therefore, the resulted circuit is always guaranteed passive network. The new method is applied to some case studies and the result verified to be properly matched in both frequency and time domain responses.**

***Keywords*: Brune's Realization Method, FDNE, Fitting, Passive Network.**

I. Introduction

TRANSIENT simulation of power systems has always been essential for accurate study of different phenomenon in the network. To get the exact and realistic simulation result, it is necessary to have tools which provide precise and stable models of power system elements. Accurate modeling of Frequency Dependent Equivalent Networks (FDNEs) in time domain has been one of the most challenging problem for the Electromagnetic Transient (EMT) programs. In this work, a new approach is introduced to obtain the time-domain model of FDNEs which guaranties accuracy and stability.

FDNEs are used to save computational resources in transient simulation of large electrical power systems or in case of modeling a black-box unidentified network. To do so, a frequency scan of the network portion either through measurement made on the actual network or via measurement on a highly detailed simulation model. The frequency scan will be stored as a table of frequency versus impedance (magnitude and phase) and then this tabular function is converted to a rational function of the Laplace transform variable '*s*' using curve-fitting methods. Finally, the rational function can readily be converted into a time domain simulation model either by RLC branches or by means of recursive convolution of exponential terms.

Marti in [1] introduced a method to model frequency dependent characteristic impedance of a transmission line in time domain. Using Bode's procedure, the tabular function has been approximated by a rational function and then expanded into partial fractions as (1).

$$Z_{eq}(s)=k_0+\frac{k_1}{s+p_1}+\frac{k_2}{s+p_2}+\cdots+\frac{k_n}{s+p_n} \quad (1)$$

The partial factions then can be readily realized by means of Foster I synthesis method which utilizes series combination of parallel RC components as it is shown in Fig. 1.

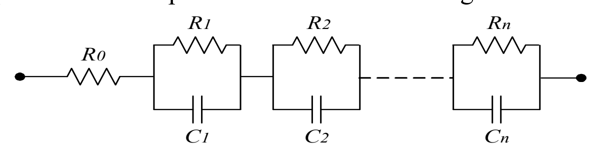

Fig. 1. Foster I equivalent circuit for frequency dependent impedance.

Where in the Fig. 1.

$$R_0=k_0 \quad , \quad R_i=k_i/p_i \quad , \quad C_i=1/k_i \quad (2)$$

Although *Marti's* method works well for smooth frequency responses, in case of many resonance peaks in the frequency response, such as with cable systems, it will cause a large number of poles and zeros and thus, makes the time domain simulation not efficient.

Gustavsen introduced a far more efficient technique to fit the non-smooth frequency responses using vector fitting [2]. This method is currently used in the majority of modern transient simulation programs. In vector fitting, the tabular function is approximated by a rational function in form of (3).

$$Y_{eq}(s)=\sum_{n=1}^{N}\frac{c_n}{s-a_n}+d+sh \quad (3)$$

Where c_n and a_n are the residues and poles respectively and can be either real quantities or complex conjugate pairs. The partial fractions then can be converted to the time domain using recursive convolution of exponential terms [3] or by means of parallel RLC branches [4] as shown in Fig. 2.

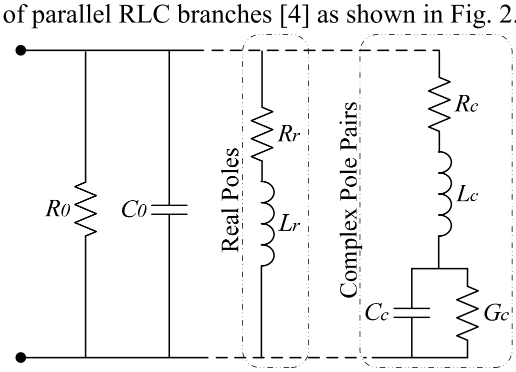

Fig. 2. RLC branches to realize real and complex pole pairs of $Y_{eq}(\omega)$.

This work was supported through the IRC Program of the Natural Sciences and Engineering Research Council (NSERC) of Canada.
M. Ahmadi and A. M. Gole are with the Power Systems Research Group, Department of Electrical and Computer Engineering, University of Manitoba, Winnipeg, MB, R3T 5V6, Canada (e-mail: ahmadim3@myumanitoba.ca).

Paper submitted to the International Conference on Power Systems Transients (IPST2017) in Seoul, Republic of Korea June 26-29, 2017

The vector fitting method sometimes results in passivity violations. It means the implemented network generates energy at some frequencies which is physically impossible. To avoid this, the fitting procedure must be closely monitored and changes enforced to ensure that the fitted function is passive. Different passivity enforcement methods have been explored in literatures [5], [6] and still being developed [7].

In this work first, *Brune's* analytical solution to realize driving point impedance of a network *Z(s)* is explained. This method inherently guaranties the passivity of the resultant circuit, and thus eliminates any requirement of passivity checking and correction as required by the main approaches in use today. Then, the idea is extended to realize a tabular function *Z(jω)* numerically. Finally, simulation result is given to verify the method.

II. Brune's Realization Method

Brune [8] in 1931 showed that the necessary and sufficient condition for the function *Z(s)* to be impedance of an RLC circuit is to be Positive Real (PR). That means, *Z(s)* must be real when *'s'* is real and real part of it must be positive when real part of *'s'* is positive. *Brune's* method uses several steps, each of which, using RLC elements realizes a portion of the passive network that represents the given PR function. The procedure ends when no further circuit is left to be realized.

The preliminary steps to realize the PR function *Z(s)* is removing all imaginary axis poles and zeros which is described as follows.

A. Step 1- Removing Imaginary Axis Poles

All the poles of *Z(s)* on imaginary axis can be removed in form of series components as (4) shows. k_∞, k_0 and k_j are the residues of the poles at infinity, zero and ω_j respectively.

$$Z(s) = k_\infty s + \frac{k_0}{s} + \sum_{j=1}^{n} \frac{2k_j s}{s^2 + \omega_j^2} + Z_1(s) \tag{4}$$

The imaginary axis poles can then be represented by a series network as depicted in Fig. 3, in series with the reminder $Z_1(s)$ which is still a PR function.

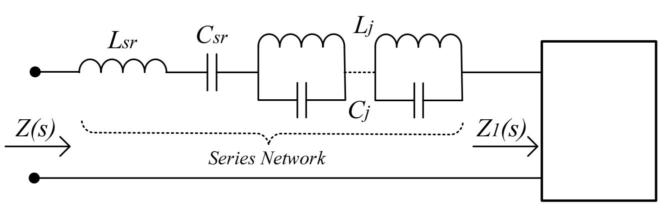

Fig. 3. Series network resulting from removing imaginary axis poles

Where comparing (4) and Fig. 3, in can be found that

$$L_{sr} = k_\infty \ , \ C_{sr} = 1/k_0 \ , \ C_j = 1/2k_j \ , \ L_j = 1/C_j\,\omega_j^2 \tag{5}$$

Then, all the imaginary axis zeros of function $Z_1(s)$ shall be removed.

B. Step 2- Removing Imaginary Axis Zeros

Zeros of the $Z_1(s)$ are the poles of function $Y_1(s)=1/Z_1(s)$. So, removing poles of $Y_1(s)$ is the same as removing zeros of $Z_1(s)$ which can be done in the same manner as part before as (6) in which $k_{\infty 1}$, k_{01} and k_i are the residues of the poles at infinity, zero and ω_i respectively.

$$Y_1(s) = 1/Z_1(s) = k_{\infty 1} s + \frac{k_{01}}{s} + \sum_{i=1}^{m} \frac{2k_i s}{s^2 + \omega_i^2} + 1/Z_2(s) \tag{6}$$

Poles of $Y_1(s)$ (or zeros of $Z_1(s)$) shall be removed as shunt components as Fig. 4 shows. Where again comparing (6) and Fig. 4, in can be found that,

$$C_{sh} = k_{\infty 1} \ , \ L_{sh} = 1/k_{01} \ , \ L_i = 1/2k_j \ , \ C_i = 1/L_i\,\omega_i^2 \tag{7}$$

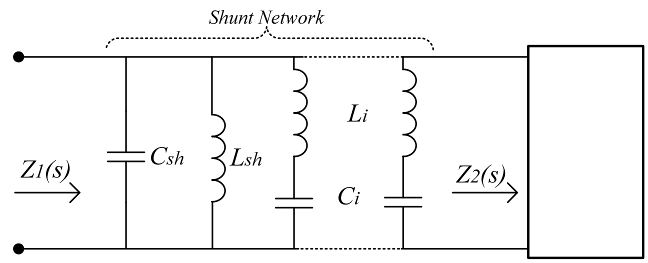

Fig. 4. Shunt network resulting from removing imaginary axis zeros

After imaginary axis poles and zeros removal by repeating the first 2 steps, a remainder function will be left which has no more poles and zeros on this axis which is called a *minimum reactance – minimum susceptance* function.

C. Step 3- Removing Minimum Real Part

Let $Z_2(s)$ be the reminder function of previous step. In this step, the minimum of real part of $Z_2(j\omega)$ is removed in form of a series resistance R_{min}.

$$Z_3(s) = Z_2(s) - R_{\min} \tag{8}$$

If this creates a zero at $f=0$ or $f=\infty$, then there will be a zero at 0 or ∞, so a zero reduction as step 2 should be done (and the zero can be removed in form of shunt elements *Lz* or *Cz*), otherwise there will be frequency ω_0 where $Z_3(j\omega_0)$ is pure imaginary. Function $Z_3(s)$ is called *minimum function* now.

D. Step 4- Brune's first cycle

As mentioned,

$$Z_3(j\omega_0) = jX \tag{9}$$

The reactance X can be removed in form of a series inductance $L_1 = X/\omega_0$.

$$Z_4(s) = Z_3(s) - sL_1 \tag{10}$$

This reduction will make a zero in $Z_4(s)$ at ω_0 which can be removed in form of a pole of $Y_4(s)$ by shunt LC component.

$$Y_5(s) = Y_4(s) - \frac{s/L_2}{s^2 + \omega_0^2} \tag{11}$$

Considering (10), there is also a pole at infinity in $Z_4(s)$ which can be realized now in form of a series inductance L_3.

$$Z_6(s) = Z_5(s) - sL_3 \tag{12}$$

Therefore, after removing the minimum real part, the *Brune's* first cycle will result in the network depicted in the Fig. 5. *Brune* has also proved that (13) is always true for the inductances L_1, L_2 and L_3. Thus, even if L_1 or L_3 may be negative, the circuit is still physically realizable by replacing the "Tee" connection with a transformer with positive leakage and mutual impedances and suitable turn's ratio.

$$L_3 = \frac{-L_1 L_2}{L_1 + L_2} \quad (13)$$

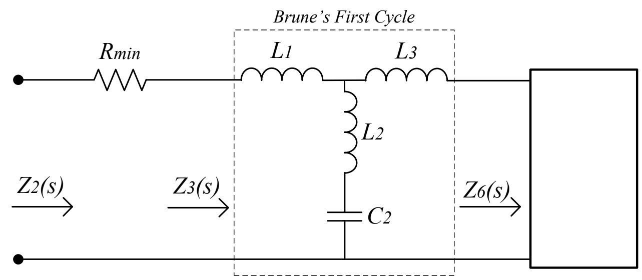

Fig. 5. Removing the minimum resistance and Brune's first cycle

Brune's first cycle will reduce the order of the impedance by two.

The above 4 steps (i.e., removing imaginary axis poles and zeros, removing minimum resistance and *Brune's* first cycle) are again applied to $Z_6(s)$ to further reduce the order of the remainder. The process is continued till the order of the resulting impedance is zero, i.e., all that remains is a resistor.

III. Numerical Implementation on Brune's Realization

In a practical application, $Z(s)$ is available as a tabulated frequency response (either magnitude and phase or real and imaginary components). The aforementioned steps in Section II above to reduce the order of the function are as follows.

A. Step 1- Removing Imaginary Axis Poles

By observing phase angle of the tabulated function, presence of poles at imaginary axis can be determined in the following way.

If the phase angle of $Z(j\omega)$ at very high frequency ω_∞ is close to +90˚, it means there is an imaginary pole at infinity. So, it can be removed in the form of series inductance. L_{sr} can be found by looking at the imaginary part of the impedance at ω_∞ while the real part must negligible.

$$L_{sr} = \frac{imag[Z(j\omega_\infty)]}{j\omega_\infty} \quad (14)$$

Likewise, if the tabulated phase angle of $Z(j\omega)$ at very low frequency ω_0 is close to –90˚, it means there is an imaginary pole at zero. So, it can be removed in form of series capacitance C_{sr}.

$$C_{sr} = \frac{imag[1/Z(j\omega_0)]}{j\omega_0} \quad (15)$$

Lastly, any sudden change in the phase angle from +90˚ to –90˚ at ω_j, means an imaginary pole at that frequency. Usually this type of poles is not very common.

$$k_j = \frac{-\omega^2 + \omega_j^2}{2j\omega} Z(j\omega) \Big|_{at\ \omega=\omega_j} \quad (16)$$

C_j and L_j of the corresponding branches can be found from k_j and ω_j as mentioned in (5). The imaginary axis poles reduction of the tabular function will be done numerically as shown in (17).

$$Z_1(j\omega) = Z(j\omega) - j\omega L_{sr} - \frac{1}{j\omega C_{sr}} - \sum_{j=1}^{n} \frac{2j\omega k_j}{-\omega^2 + \omega_j^2} \quad (17)$$

B. Step 2- Removing Imaginary Axis Zeros

Also, observing the phase angle of tabulated function gives information of imaginary zero. For example, If the phase angle of $Z(j\omega)$ at very high frequency ω_∞ is close to –90˚, it means there is an imaginary zero at infinity. The imaginary axis zeros of $Z_1(j\omega)$ will be removed in form of poles of $Y_1(j\omega)$ with the same procedure as mentioned before by investigating the behaviors of phase angle at very high and very low frequencies and also sudden changes from +90˚ to –90˚. Then these poles can be removed numerically as

$$1/Z_2(j\omega) = Y_1(j\omega) - j\omega C_{sh} - \frac{1}{j\omega L_{sh}} - \sum_{i=1}^{m} \frac{2j\omega k_i}{-\omega^2 + \omega_i^2} \quad (18)$$

C_i and L_i of the corresponding branches can be found from k_i and ω_i as mentioned in (7).

C. Step 3- Removing Minimum Real Part

The minimum of real part of $Z_2(j\omega)$ is can be easily found by looking into the tabular function and can be removed in form of a series resistance R_{min}.

$$Z_3(j\omega) = Z_2(j\omega) - R_{\min} \quad (19)$$

Likewise, the analytical one, if this removal creates a zero at $f=0$ or $f=\infty$, the situation is similar to what happened in step 2 (and the zero can be removed in form of shunt elements *Lz* or *Cz*). If not, there will be frequency ω_0 where $Z_3(j\omega_0)$ is pure imaginary.

D. Step 4- Brune's First Cycle

Same as before, the *Brune's* first cycle can be applied numerically. So, if

$$Z_3(j\omega_0) = jX \quad (20)$$

Then reactance X will be removed in form of a series inductance L_1.

$$Z_4(j\omega) = Z_3(j\omega) - j\omega L_1 \quad (21)$$

The zero in $Z_4(j\omega)$ at ω_0 will be removed in form of a pole of $Y_4(j\omega)$ by shunt LC component.

$$Y_5(j\omega) = Y_4(j\omega) - \frac{j\omega / L_2}{-\omega^2 + \omega_0^2} \quad (22)$$

Also, the pole at the infinity in $Z_4(j\omega)$ will be realized in form of a series inductance L_3.

$$Z_6(j\omega) = Z_5(j\omega) - j\omega L_3 \quad (23)$$

The 4 steps will be repeated till the phase angle of the reminder impedance becomes almost zero in all frequencies. This means there is a constant impedance which can be modeled by a resistor.

IV. Simulation Result

The functionality of the new approach of fitting is verified trough out study of three different scenarios. The proposed method always guarantees the passivity of the realized network. However, at this stage, comparison of its performance with other methods, i.e., examples where vector fitting produces non-passive results has not been investigated and is left for future work.

A. Simple PR Function

As of first scenario, the following simple function of frequency is examined using *Brune's* "analytical" solution. Then the function is calculated in a range of frequency and the tabulated function is fitted "numerically" using proposed method.

$$Z(s)=\frac{1.5s^2+4.5s+9.5}{s^2+s+1} \tag{24}$$

The presence of poles and zeroes can be determined in numerical method by observing the phase angle at very low and very high frequencies. In this example, it approaches zero at both very low and very high frequencies which means there are no imaginary poles or zeros. The next step will be removing the minimum real part of $Z(j\omega)$ which results in a resistance of 0.5Ω at $\omega_0=1.732\approx\sqrt{3}$.

$$Z_3(s)=\frac{1.5s^2+4.5s+9.5}{s^2+s+1}-0.5=\frac{s^2+4s+9}{s^2+s+1} \tag{25}$$

Then, inductance L_1 of *Brune's* first cycle will be realized as:

$$L_1=\frac{Z_3(j\omega_0)}{\omega_0}=\frac{1}{\sqrt{3}}\frac{(j\sqrt{3})^2+4j\sqrt{3}+9}{(j\sqrt{3})^2+j\sqrt{3}+1}=\frac{-j2\sqrt{3}}{\sqrt{3}}=-2\ H \tag{26}$$

Now, this inductance can be removed which creates a zero at ω_0 in the remaining impedance;

$$Z_4(s)=\frac{s^2+4s+9}{s^2+s+1}-(-2s)=\frac{2s^3+3s^2+6s+9}{s^2+s+1} \tag{27}$$

The zero of $Z_4(s)$ will be realized in form of a pole of admittance $Y_4(s)$ utilizing a shunt LC branch. To find the residue of this pole;

$$\frac{1}{L_2}=\frac{s^2+\omega_0^2}{s}Y_4(s)\Big|_{s=j\omega_0}=\frac{1}{s}\frac{s^2+s+1}{2s+3}\Big|_{s=j\sqrt{3}}=\frac{1}{3} \tag{28}$$

Which means $L_2=3H$, and this also gives;

$$C_2=\frac{1}{\omega_0^2 L_2}=\frac{1}{9}F \tag{29}$$

Then, removing this pole from the admittance $Y_4(s)$,

$$Y_5(s)=Y_4(s)-\frac{s/L_2}{s^2+\omega_0^2}=\frac{1}{6s+9} \tag{30}$$

Then we can realize L_3 in *Brune's* first cycle using (13) which results an inductance $L_3=6H$.

Finally, removing L_3 will gives a remainder constant impedance, i.e., a 9Ω resistance.

$$Z_6(s)=Z_5(s)-sL_3=6s+9-6s=9\Omega \tag{31}$$

Fig. 6 shows the realized circuit and it can be seen that the analytical solution using *Brune's* method (the red quantities on the figure) is almost the same as numerical solution.

Fig. 7 also shows the frequency response of the original function comparing to the realized circuit. The two responses agree very well as it was expected from the resulted circuits. Deviation is not depicted as it was less than 0.014%.

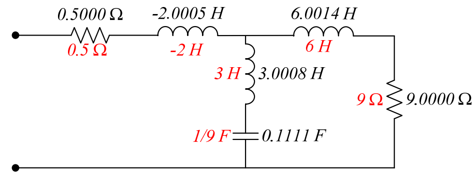

Fig. 6 The fitted circuit using analytical solution (red) and the proposed method (black).

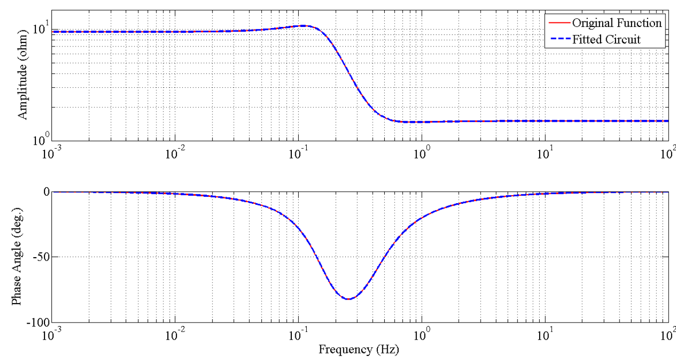

Fig. 7 Frequency response of the original function and the fitted circuit.

B. Higher Order PR Function

The second scenario is to fit an arbitrary high order PR function. A network scan was performed on a passive network. To do so, a 17th order rational function has been scanned in frequency domain. The function is presumed to be in form of (32).

$$Z(s)=\sum_{n=1}^{N}\frac{c_n}{s-a_n}+d+sh \tag{32}$$

Which poles and zeros of the function is prescribed in Table I.

TABLE I
POLES AND RESIDUES OF THE 17TH ORDER POSITIVE REAL FUNCTION

Poles (rad/sec)		Residues (ohm.rad/sec)	
– 4500		+ 3000	
– 120	± j1500	– 250	± j18
– 300	± j45000	– 6000	± j155
– 70	± j50	– 50	± j70
– 500	± j9000	– 1400	± j60
– 90	± j1000	– 1550	± j31000
– 80000	± j5000	– 5000	± j70000
– 40000	± j450	– 800	± j150000
– 20000	± j5000	– 10000	± j1500000
$d=0.2$ and $h=0$			

The above function was tabulated at 10000 data points and then was fitted with an equivalent circuit using the proposed method.

Fig. 8 shows the configuration of the realized circuit using the proposed method. Only one block is shown due to space limitation, but there are total of 12 cascaded blocks terminated by R_{end} which is the aforementioned constant impedance at the end.

For the given 17th order PR function, quantities of the circuit's elements are realized as specified in Table II.

TABLE II

QUANTITIES OF EACH ELEMENT IN EACH BLOCK OF THE REALIZED CIRCUIT OF THE 17TH ORDER POSITIVE REAL FUNCTION.

	Block #											
	1	**2**	**3**	**4**	**5**	**6**	**7**	**8**	**9**	**10**	**11**	**12**
L_{sr} (H)	0	0	0	2.255e-9	0	0	0	0	0	0	0	0
R_{min}(Ω)	7.659e-4	0.0726	0.0128	0	0.0248	0.1457	0.0090	0.0966	0.4183	0.0341	0.0587	0.0382
L_z (H)	∞	∞	∞	∞	∞	∞	∞	∞	∞	0.0136	∞	∞
C_z (F)	0	0	9.101e-6	0	0	0	0	0	0	0	0.0014	0.0077
L_1 (H)	5.547e-5	2.232e-8	0	0	4.973e-6	1.264e-5	2.280e-6	5.535e-5	3.668e-4	0	0	0
C_2 (F)	1.100e-4	7.531e-7	0	0	4.272e-6	1.058e-4	1.105e-5	2.080e-4	0.0015	0	0	0
L_2 (H)	1.067e-4	6.608e-7	∞	∞	1.026e-5	1.460e-5	4.026e-5	8.149e-5	4.936e-4	∞	∞	∞
L_3 (H)	-3.65e-5	-2.16e-8	0	0	-3.35e-6	-6.78e-6	-2.16e-6	-3.30e-5	-2.10e-4	0	0	0
R_{end}(Ω)	0.63966											

TABLE III

QUANTITIES OF EACH ELEMENT IN EACH BLOCK OF THE REALIZED CIRCUIT OF THE REALISTIC NETWORK.

	Block #												
	1	**2**	**3**	**4**	**5**	**6**	**7**	**8**	**9**	**10**	**11**	**12**	**13**
R_{min}(Ω)	1.9895	1.9749	2.0602	0.2033	24.828	2.8615	6.7948	13.825	11.359	1.8787	11.281	2.8260	4.3591
L_z (H)	∞	∞	∞	∞	∞	∞	∞	∞	∞	0.0745	0.0883	∞	∞
L_1 (H)	-0.0020	-0.0054	1.35e-4	-0.0055	0.0314	0.0333	0.0075	0.0175	8.36e-4	0	0	0.0014	6.94e-4
C_2 (F)	4.29e-7	6.36e-7	1.64e-6	1.59e-6	4.13e-6	2.97e-5	2.98e-6	1.52e-5	1.88e-6	0	0	1.57e-6	1.76e-6
L_2 (H)	0.0212	0.1013	0.0103	0.0570	0.0860	0.083	0.0470	0.0665	0.0397	∞	∞	0.0283	0.0163
L_3 (H)	0.0022	0.0058	-1.3e-4	0.006	-0.0230	-0.0238	-0.0065	-0.0139	-8.2e-4	0	0	-0.0013	-6.7e-4
R_{end}(Ω)	14.8097												

There are some missing elements from the circuit of Fig. 8 in the table which means they have not happened in the realizing process.

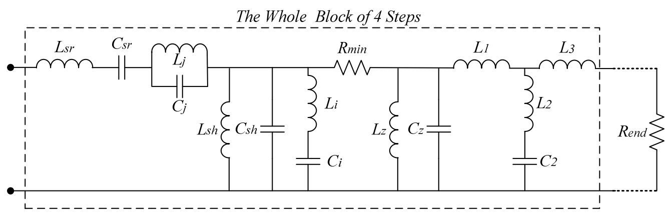

Fig. 8. The realized circuit's configuration.

Fig. 9 shows the response of the original function and the response of the fitted circuit in frequency domain as well as the deviation of the two. It can be seen that both amplitude and the phase angle of the fitted circuit agree the original function very well.

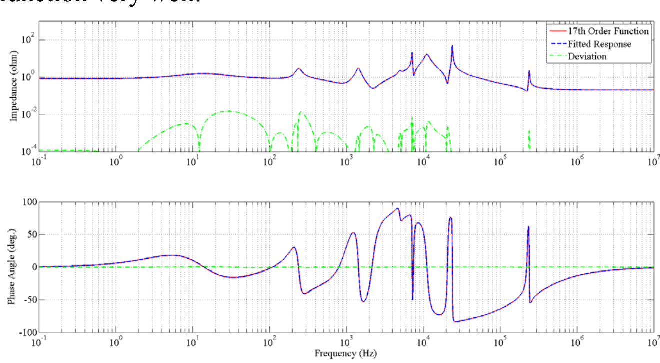

Fig. 9. Frequency response of the fitting result from the proposed method comparing with the original function.

C. Fitting a Realistic Network

In the third scenario, a more realistic network which is shown in Fig.10 was modeled. The data is given in the Appendix. The figure shows a 22kV source connected to a 100 remote loads with a 100km long cable. A filter bank is also present. The frequency response (FDNE) of this network was tabulated using a frequency scan in a time-domain simulator (PSCAD) module from the Fault terminal point of view. Then using the proposed method, the FDNE of the network is reduced.

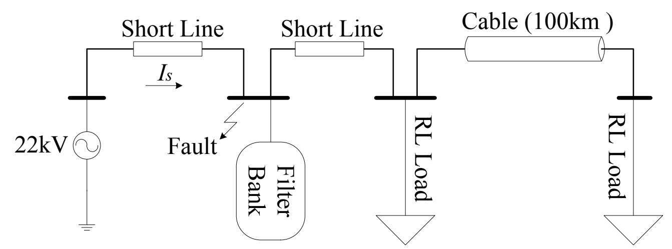

Fig. 10 The more realistic example showing the network and the fault location and the sending end current (*Is*). Data is in the appendix

Fig. 11 shows the frequency response of the two circuits from the point of coupling. It can be seen that the fitted circuit response is very close to the original one.

The realized circuit will have 13 blocks of the type shown in Fig. 8 with the quantities given in Table III. In this table also those missing elements of Fig. 8 have not happened in the realizing process.

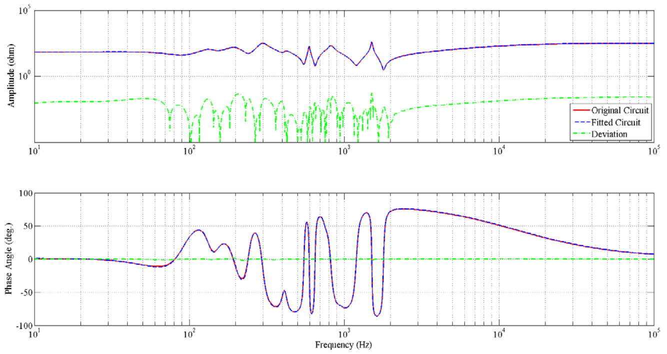

Fig. 11. Frequency response of the fitting result from the proposed method comparing with the original circuit's response.

In this scenario, to verify the fitting result in the time domain simulation (PSCAD), both of the original circuit and the fitted one are examined in both transient and steady state situation after applying a fault. Fig. 12 is the sending end current I_s, which shows the initial transient and then the settling to steady state after fault application at 0.12 seconds and fault clearance at 0.18 seconds. The time domain responses of the two circuits also are essentially identical.

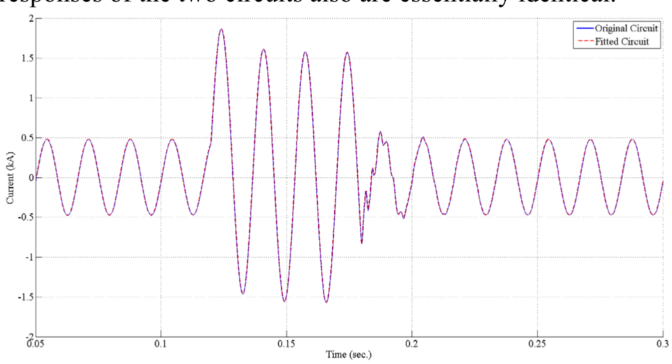

Fig. 12. Sending end current of the original circuit comparing to the fitted circuit during and after applying fault, simulated in PSCAD.

From the simulation speed point of view, the original circuit has a CPU runtime of 577 *ms* and the fitted circuit results in 124 *ms* which means it could reasonably reduce the network size and speed up the simulation. As of now, the FDNE was directly implemented in PSCAD. Further time savings are likely possible if the FDNE is modelled as an external module using a nested and fast simultaneous solution as reported in [9] and [10]. This is planned for future work.

V. Appendix: Example System Data

Small T-line sections modelled as L-R circuits:
L=50 *mH, R* =5 Ω
RL Loads:
R = 125 Ω*, L* =180 *mH*
Filters: 1 *MVAR* equally distributed between 3rd, 11th/13th double tuned and 24th/26th double tuned HP filters.
Cable:
Resistivity = 1.68e-8 Ω.m, *Relative Permittivity* = 4.1 and *Relative Permeability* = 1.

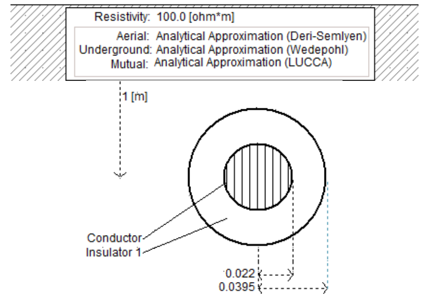

Fig. 13 Cross section of the cable buried 1 meter underground.

VI. Conclusion

In this paper, a new approach of fitting the frequency response of the FDNEs has been presented. In this method, the frequency scan can be directly transferred to the time domain simulation by means of an RLC network with the same frequency response. This new technique is a numerical extension to the *Brune's* network realization method which guarantees passivity of the resulted circuit in all range of the frequencies. Thus, there will not be any instability problem whatsoever due to violation of passivity. It is shown that the *Brune's* synthesis method can be implemented algorithmically and coded easily in simulation tools. Verification of the method is done by some case studies both in time domain and frequency domain and the results are shown to be very closely matched. The new fitting method also increased the time domain simulation speed comparing the original network.

VII. References

[1] J.R. Marti, "Accurate Modelling of Frequency-Dependent Transmission Lines in Electromagnetic Transient Simulations", *IEEE Trans. Power Apparatus and Systems*, vol. 101, no. 1, pp. 147-157, Jan. 1982.

[2] B. Gustavsen and A. Semlyen, "Rational Approximation of Frequency D omain Responses by Vector Fitting", *IEEE Trans. Power Delivery*, vol. 14, no. 3, pp. 1052-1061, July 1999.

[3] A. Semlyen and A. Dabuleanu, "Fast and accurate switching transient calculations on transmission lines with ground return using recursive convolutions," *IEEE Trans. Apparatus and Systems*, vol. PAS-94, pp. 561– 571, Mar. /Apr. 1975.

[4] B. Gustavsen, "Computer code for rational approximation of admittance matrices", *IEEE Trans. Power Delivery*, vol. 17, no. 4, pp. 1093-1098, Oct. 2002.

[5] B. Gustavsen and A. Semlyen, "Enforcing passivity for admittance matrices approximated by rational functions," *IEEE Trans. Power Systems*, vol. 16, pp. 97-104, Feb. 2001.

[6] B. Gustavsen, "Fast passivity enforcement for pole-residue models by perturbation of residue matrix eigenvalues," *IEEE Trans. Power Delivery*, vol. 23, no. 4, pp. 2278–2285, Oct. 2008.

[7] Y. Hu, W. Wu and B. Zhang, "A Semidefinite Programming Model for Passivity Enforcement of Frequency-Dependent Network Equivalents," *IEEE Trans. Power Delivery*, vol. 31, no. 1, pp. 397–399, Feb. 2016.

[8] O. Brune, "Synthesis of a finite two-terminal network whose driving-point impedance is a prescribed function of frequency," *Journal of Mathematics and Physics*, vol. 10, pp. 191–236, Apr. 1931.

[9] U. N. Gnanarathna, A. M. Gole and R. P. Jayasinghe, "Efficient Modeling of Modular Multilevel HVDC Converters (MMC) on Electromagnetic Transient Simulation Programs," *IEEE Trans. Power Delivery*, vol. 26, no. 1, Jan 2011.

[10] K. Strunz and E. Carlson, "Nested Fast and Simultaneous Solution for Time-Domain Simulation of Integrative Power-Electric and Electronic Systems," *IEEE Trans. Power Delivery*, vol. 22, no. 1, Jan 2007.